Eur. J. Biochem. **265**, 430–440 (1999) © FEBS 1999

Type I β-turn conformation is important for biological activity of the melanocyte-stimulating hormone analogues

Song-Zhe Li[1], Jung-Hoon Lee[2], Weontae Lee[2], Chang-Ju Yoon[3], Ja-Hyun Baik[4] and Sung-Kil Lim[1]

[1]*Department of Internal Medicine, College of Medicine, Yonsei University, Seoul, Korea;* [2]*Department of Biochemistry, College of Science, Yonsei University, Seoul, Korea;* [3]*Department of Chemistry, College of Science, Catholic University, Seoul, Korea;* [4]*Clinical Research Center, College of Medicine, Yonsei University, Seoul, Korea*

In order to define which structure of α-melanocyte-stimulating hormone (MSH) analogues plays a critical role for ligand–receptor interaction and selectivity, we analysed receptor-binding and cAMP-generating activity in Chinese hamster ovary cell lines stably transfected with rMC3R and hMC4R, as well as the NMR structures of chemically synthesized α-MSH analogues. Compared with [Ahx4]α-MSH, the linear MTII designated as α-MSH-ND revealed a preference for the MC4R, whereas its IC_{50} and EC_{50} values were comparable to those of MTII reported previously. Truncation of Ahx4 and Asp5 of α-MSH-ND remarkably decreased the receptor-binding and cAMP-generating activity. Meanwhile, maximum cAMP-generating activity was observed at a higher concentration (10^{-5} M) of α-MSH-ND(6–10), and MC4R preference was changed into MC3R preference. In contrast, [Gln6]α-MSH-ND(6–10) lost its cAMP-generating activity almost completely, even though it bound to both receptors. Whereas the solution conformation of α-MSH-ND revealed a stable type I β-turn structure, [Gln6]α-MSH-ND(6–10) revealed a tight γ-turn composed of Gln6-D-Phe7-Arg8. Replacement of the His6 residue of α-MSH-ND by Gln, Asn, Arg or Lys decreased not only the receptor binding, but also the cAMP-generating activity in both the MC3R and the MC4R. The structure of [Gln6]α-MSH-ND exhibited a stable type I′ β-turn comprising Asp5, Gln6, D-Phe7 and Arg8. [Lys6]α-MSH-ND showed a greatly reduced binding affinity and cAMP-generating activity with the loss of MC4R selectivity. In NMR studies, [Lys6]α-MSH-ND also demonstrated a γ-turn conformation around Lys6-DPhe7-Arg8. From the above results, we conclude that a type I β-turn conformation comprising the residues Asp5-His6-(D-Phe7)-Arg8 was important for receptor binding and activation, as well as the selectivity of MSH analogues.

Keywords: melanocortin; melanocyte-stimulating hormone receptor; NMR; receptor-binding and cAMP-generating activity; type I β-turn.

The peptide hormone precursor pro-opiomelanocortin (POMC) is cleaved post-translationally to give rise to a variety of biologically active substances called melanocortins [1], including α-, β-, and γ-melanocyte stimulating hormones (MSH) and adrenocorticotropin. POMC gene expression is limited to ARC (arcuate) neurones that project to areas that express melanocortin receptors and participate in energy homeostasis. As leptin receptors are expressed on POMC neurones, melanocortin neurones appear to be a target of leptin action [2]. Over the past several years, molecular cloning of the five melanocortin receptor subtypes (MC1R–MC5R) has also provided the tools for systemic studies of the molecular mechanisms of their physiologic effects [3–7].

Mutations of the POMC gene in humans [8] or the MC4R gene in mice [9] have resulted in obesity, whereas the overexpression of agouti or agouti-related protein has also induced obesity in mice [10,11]. Agonists of melanocortin receptors elicit anorexia, whereas antagonists have the opposite effect. Activation of the MC4R by α-MSH increases the energy expenditure, decreases the food intake, and promotes sympathetic activity [12]. All of these findings, directly or indirectly, have provided evidence that melanocortin is involved critically in the control of food intake and body weight homeostasis, and that it could reduce adiposity in patients with obesity [13,14]. As melanocortin has catabolic effects, its analogue has been listed as one of the target molecules for the medical treatment of obesity. Until now, most α-MSH analogues have preferably bound to the MC3R and the MC4R with high affinity. However, if melanocortin analogues are to be developed as anti-obesity medicine, then one that is MC4R-selective and has the least systemic side-effects will be better, and it should preferably be developed as a small organic compound to pass the blood–brain barrier easily. Therefore, the structural and functional studies of α-MSH analogues are critically important for the development of potent α-MSH analogues satisfying the above requirements.

Correspondence to S.-K. Lim, Division of Endocrinology, Department of Internal Medicine, College of Medicine, Yonsei University, Shinchon-Dong, Seodaemun-Gu, 120-752 Seoul, Korea.
Fax: +82 2 393 6884, Tel.: +82 2 361 5432,
E-mail: lsk@yumc.yonsei.ac.kr

Abbreviations: POMC, pro-opiomelanocortin; MSH, melanocyte stimulating hormone; Ahx, α-aminohexanoic acid; NDP-MSH, [Ahx4, D-Phe7]α-MSH; MTII, melanotan II; α-MSH-ND, Ac–Ahx4–Asp5-His6-(D-Phe7)-Arg8-Trp9-Lys10-NH_2; MC3R, melanocortin-3 receptor; MC4R, melanocortin-4 receptor; ARC, arcuate nucleus; CHO, Chinese hamster ovary cell line; FBS, foetal bovine serum; REM, restraint energy minimization; TOCSY, total correlation spectroscopy; ROE, rotating-frame Overhauser effect; NOESY, nuclear Overhauser effect spectroscopy; DG, distance geometry; SA, simulated-annealing; DQF-COSY, double-quantum-filtered correlated spectroscopy; RIA, radioimmunoassay.

(Received 7 April 1999, revised 12 July 1999, accepted 29 July 1999)

NDP-MSH with a seven-lactam-ring structure has been known as the most potent melanocortin agonist [15]. The substitution of Phe7 in α-MSH to D-Phe7 increased the receptor-binding and cAMP response, as well as MC4R selectivity [16,17]. Furthermore, the substitution of D-Phe7 for Phe7 provided the insight that the core structure of α-MSH analogues is critically important for ligand–receptor interaction and selectivity [18]. Recently, we reported that α-MSH forms a hairpin loop conformation, whereas α-MSH-ND prefers a type I β-turn structure comprising the residues of Asp5-His6-(D-Phe7)-Arg8 [19]. To study further the functional importance of the type I β-turn structure and to provide direction for the future development of α-MSH analogues, we generated several α-MSH analogues by not only deleting the Ahx 4 and Asp5 residues of α-MSH-ND, but by also substituting the His6 residue of α-MSH-ND with Gln, Asn, Arg or Lys. These analogues were analysed for their receptor-binding and cAMP-generating ability in Chinese hamster ovary (CHO) cell lines stably transfected with rMC3R and hMC4R, and for their NMR spectroscopy. Here, we suggest which structure is important for receptor binding and activation as well as the selectivtiy of these α-MSH analogues.

EXPERIMENTAL PROCEDURES

Chemicals

All media and sera for cell cultivation were purchased from Gibco-BRL. NDP-MSH and other chemicals were purchased from Sigma unless specified otherwise.

Peptides synthesis

The peptides used in this study (except NDP-MSH) were synthesized at the Korea Basic Science Institute (Seoul, Korea) by use of the solid phase approach and purified by HPLC. The peptide sequences were assembled with a Milligen 9050 (Fmoc Chemistry). The correct molecular masses of the peptides were confirmed by MS. For deprotection, a reagent mixture (88% trifluoroacetic acid, 5% phenol, 2% triisopropylsilane, 5% H_2O; 2 h) was used. The raw peptides formed were purified by HPLC (Delta PAK 15μ C18 300 Å 3.9 × 150 mm column, detection at 240 nm).

Expression of melanocortin receptor clones and cell culture

Both rat MC3R and human MC4R cDNA were cloned into the expression vector pcDNAI neo. For receptor expression, CHO cells were grown in F-12 medium with 10% foetal bovine serum (FBS) and 95% O_2 air/5% CO_2 and transfected with rMC3R- and hMC4R-pcDNAI neo, respectively, by a calcium phosphate method. Briefly, 5–7 × 10^5 cells (approximately 80% confluent cultures) were plated per 10-cm culture dish the day before they were transfected. Cells were fed with flash complete culture medium containing 20 mM Hepes and incubated at 95% O_2 air/5% CO_2. After 3–4 h, the medium was discarded and 5 mL calcium phosphate-DNA precipitate containing 25 μg DNA, 124 mM $CaCl_2$, 140 mM NaCl, 25 mM Hepes and 1.41 mM Na_2HPO_4 (pH 7.12) was added. The cells were then incubated for 4 h with 97% O_2 air/3% CO_2, washed with NaCl/P_i (137 mM NaCl, 2.68 mM KCl, 4.3 mM N_2HPO_4, 1.47 mM KH_2PO_4, pH 7.12), and shocked with glycerol buffer (15% glycerol, 140 mM NaCl, 25 mM Hepes and 1.41 mM Na_2HPO_4, pH 7.12), washed again with NaCl/P_i, and incubated for an additional 36–48 h in complete F-12 medium. Cells were then cultured in complete F-12 medium containing 0.5 mg·mL^{-1} G418 (Geneticin; Life Technologies) until G418-resistant colonies appeared. G418-resistant colonies were picked out and subcultured for at least 10–14 days. Rat MC3R- and human MC4R-expressing cells were identified by screening more than 15 colonies and confirmed by assay of [Ahx4]α-MSH-induced cyclic AMP accumulation and agonist-induced inhibition of iodinated NDP-MSH binding to receptors.

Binding study

Iodinated NDP-MSH, [^{125}I](iodotyrosyl^2)-[Ahx4, D-Phe7] α-MSH, was prepared by the modified chloramine-T method as follows: 1 mCi (10 μL) Na[^{125}I] (Amersham) was added to 5 μg NDP-MSH in 100 μL 200 mM sodium phosphate buffer (pH 7.2); 20 μL 2.8 mg·mL^{-1} chloramine T solution in 200 mM sodium phosphate (pH 7.2) was then added for 15 s at which time the reaction was stopped with 50 μL of 3.6 mg·mL^{-1} sodium metabisulfate. The reaction mixture was then diluted in 1 mL of 0.1% BSA containing 0.1% trifluoroacetic acid and purified by C18 Sep-Park cartridge (Waters) and Sephadex G25 Gel Filtration Chromatography; 100 μL 0.1% BSA was added to all fractions containing radioactivity. For binding assays, the stably transfected CHO cells were plated 48 h before experiments in 24-well culture plates (Falcon Plastics) at a density of 5 × 10^4 per well until they were 90–95% confluent on the day of assay. Maintenance media was removed and the cells were washed twice with washing buffer (50 mM Tris/HCl, 100 mM NaCl, 5 mM KCl, 2 mM $CaCl_2$, pH 7.2), and immediately incubated at 37 °C for 2 h with 0.25 mL binding buffer (containing 50 mM Tris/HCl, 100 mM NaCl, 5 mM KCl, 2 mM $CaCl_2$, 5% Hanks' Balanced Salt Solution, 0.5% BSA, pH 7.2) in each well containing a constant concentration of [^{125}I]NDP-MSH and appropriate concentrations of the competing unlabelled ligand. At the end of incubation, the plates were placed on ice for 15 min and the cells were washed twice with 0.5 mL ice-cold binding buffer and then detached from the plates using 0.5 mL 0.05 M NaOH twice (final volume, 1 mL). Radioactivity was determined (Workman automatic gamma counter) and data were analysed with a software package suitable for radioligand binding data analysis (GraphPad Prism Programme). Nonspecific binding was determined by measuring the amount of [^{125}I]NDP-MSH remaining bound in the presence of 10^{-5} M unlabelled NDP-MSH, and specific binding was calculated by subtracting nonspecifically bound radioactivity from total bound radioactivity. IC_{50} (nM) values were reported as mean ± SE. All binding assays were performed in triplicate wells and repeated twice.

Cyclic AMP assay

The CHO cells expressing the receptors were grown to confluence in 24-well plates. Cell culture medium was changed to complete F-12 medium containing 10% FBS 3–4 h before cells were treated with peptides. For assays, the medium was removed and cells were washed with 0.5 mL cAMP-generating medium containing 10% FBS, 2 mM 3-isobutyl-1-methyl-xanthine, 0.1% BSA, 20 mM Hepes, 0.002% ascorbic acid in complete F-12 Medium. cAMP-generating media (0.25 mL) containing various concentrations of peptides were added and the cells were incubated for 30 min at 37 °C. The media were then discarded completely, and cells were frozen at −70 °C for 30 min and thawed at room temperature for 15–20 min. The process of freeze–thawing was repeated twice more.

Subsequently, the cells were detached from the plates with 1 mL 50 mM HCl solution per well, transferred to a 1.5-mL Eppendorf tube, followed by a 10 min centrifugation at 1900 × g. The supernatant was diluted 50-fold with radioimmunoassay (RIA) buffer and cAMP concentration was measured by cAMP ^{125}I RIA Kit (INCSTAR) according to the manufacturer's instructions. The mean values of the data were fit to a sigmoid curve with a variable slope factor using the nonlinear squares regression in a GRAPHPAD PRISM. EC_{50} (nM) values were described as mean ± SE. All of the cAMP assays were performed in triplicate wells and repeated twice. Student's *t*-test was used to determine the statistical significance of changes in binding affinity and the potency of the peptides ($P < 0.05$ was considered significant).

Preparation of NMR samples

Three α-MSH analogues, [Gln6]α-MSH-ND, [Gln6]α-MSH-ND (6–10) and [Lys6]α-MSH-ND were dissolved in 90% H_2O/10% D_2O or 99.99% D_2O at pH 7.0 with 50 mM sodium phosphate buffer. NMR samples with D_2O were prepared after lyophilization of an H_2O sample. The final sample concentrations for NMR measurements were 2 mM in 0.5 mL buffer solution.

NMR

NMR was carried out at 10, 20 and 30 °C on a Bruker DRX-500 spectrometer equipped with a triple resonance probe having x,y,z gradient coils. Most NMR spectra were recorded at 10 °C and some experiments were also recorded at 20 °C and 30 °C to calculate temperature coefficients. Pulsed-field gradient techniques were used for all H_2O experiments, resulting in good suppression of the solvent signal. Two-dimensional total correlation spectroscopy (TOCSY) [20] with MLEV-17 mixing pulse of 69.7 ms and two-dimensional nuclear Overhauser effect spectroscopy (NOESY) [21] using 100–600 ms mixing times were performed. Two-dimensional rotating-frame Overhauser effect spectroscopy (ROESY) spectra with 100–800 ms ROE mixing times was also recorded in D_2O solution. Two-dimensional double-quantum-filtered (DQF) COSY spectra [22] were collected in H_2O to obtain a vicinal coupling constant. A series of one-dimensional NMR measurements was made to identify slowly exchanging amide hydrogen resonances on a freshly prepared D_2O solution after lyophilization of a H_2O sample. All NMR experiments were performed in the phase-sensitive mode using the time proportional phase incrementation method [23] with 2048 data points in the t_2 and 256 in the t_1 domain.

All NMR data were processed using nmrPipe/nmrDraw (Biosym/Molecular Simulations, Inc.) or XWINNMR (Bruker Instruments) software. Processed data were analysed using SPARKY 3.60 developed at UCSF on a Silicon Graphics Indigo^2 workstation. Prior to Fourier transformation in the t_1 dimension, the first row was half-weighted to suppress t_1 ridges [24]. DQF-COSY data were processed to 8192 × 1024 matrices to obtain maximum digital resolution for coupling constant measurements. The proton chemical shifts were referenced with internal sodium 4,4-dimethyl-4-silapentane 1-sulfonate.

Structure calculations

The hybrid distance geometry and dynamical simulated-annealing protocol with the XPLOR 3.81 (Biosym/Molecular Simulations, Inc.) program on a Silicon Graphics Indigo^2 workstation were used for structure calculations [25,26]. Distance geometry (DG) substructures were generated using a subset of atoms and followed a refinement protocol described in Lee *et al*. [27]. The target function for molecular dynamics and energy minimization consisted of covalent structure, van der Waals' repulsion, NOE and torsion angle constraints. Based on cross-peak intensities in the NOESY/ROESY spectra with mixing times of 100–600 ms, the distance constraints were classified into three distance ranges: strong (0.18–0.27 nm), medium (0.18–0.33 nm) and weak (0.18–0.50 nm). Pseudo-atom corrections were also used for nonstereospecifically assigned methylene protons, methyl groups and the ring protons of phenylalanine residue [28]. The NOESY spectra of [Gln6]α-MSH-ND, [Gln6]α-MSH-ND(6–10) and [Lys6] α-MSH-ND yielded 58, 49 and 50 NOE constraints, respectively. Constraints for the dihedral angles for all peptides were also deduced on the basis of the $^3J_{HN\alpha}$ coupling constants from two-dimensional DQF-COSY spectra in H_2O.

RESULTS

We designed and synthesized a series of new linear MSH analogues in which the structures are aligned with NDP-MSH and α-MSH-ND (Table 1). The rat MC3R DNA and human MC4R DNA were stably and independently expressed in CHO cells for competitive receptor binding with [^{125}I]NDP-MSH as a radioligand and a cyclic AMP accumulation test following treatment with different ligands.

Table 1. Alignment of α-MSH, NDP-MSH, linear MTII(α-MSH-ND) with the new analogues evaluated in this study. All peptides have an acetyl-group on the N terminus and an amide group on the C terminus. The main substituted amino acid residues are shown in italics.

	Position												
Peptide	1	2	3	4	5	6	7	8	9	10	11	12	13
[Ahx4] α-MSH	Ser	Tyr	Ser	Ahx	Glu	His	Phe	Arg	Trp	Gly	Lys	Pro	Val
NDP-MSH	Ser	Tyr	Ser	Ahx	Glu	His	D-Phe	Arg	Trp	Gly	Lys	Pro	Val
α-MSH-ND				Ahx	Asp	His	D-Phe	Arg	Trp	Lys			
[Gln6]α-MSH-ND				Ahx	Asp	*Gln*	D-Phe	Arg	Trp	Lys			
[Asn6]α-MSH-ND				Ahx	Asp	*Asn*	D-Phe	Arg	Trp	Lys			
[Arg6]α-MSH-ND				Ahx	Asp	*Arg*	D-Phe	Arg	Trp	Lys			
[Lys6]α-MSH-ND				Ahx	Asp	*Lys*	D-Phe	Arg	Trp	Lys			
α-MSH-ND(6–10)						His	D-Phe	Arg	Trp	Lys			
[Gln6]α-MSH-ND(6–10)						*Gln*	D-Phe	Arg	Trp	Lys			
[Asn6]α-MSH-ND(6–10)						*Asp*	D-Phe	Arg	Trp	Lys			

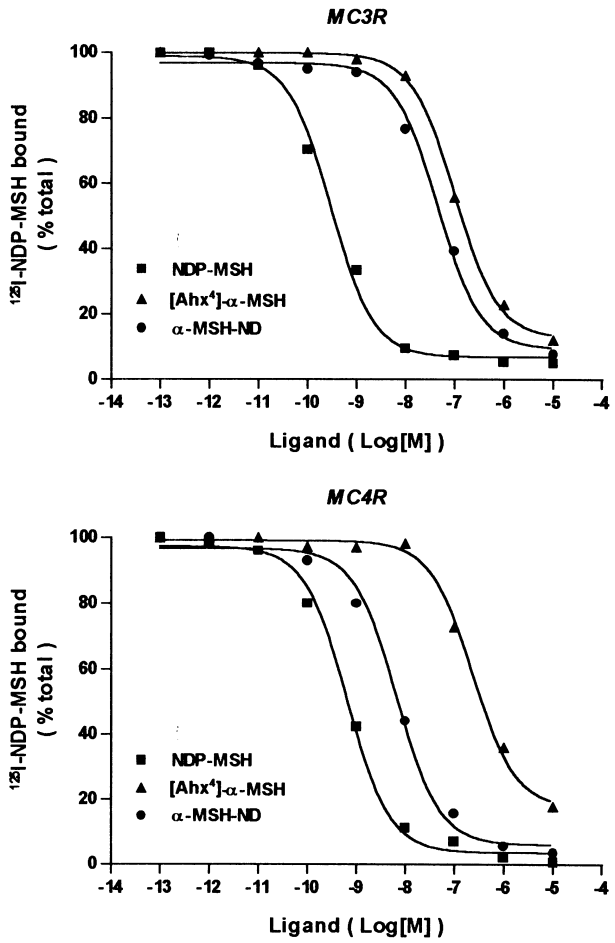

Fig. 1. Competition curves of α-MSH analogues obtained in CHO cell lines stably transfected with MC3R and MC4R using a fixed concentration of [^{125}I]NDP-MSH and varying concentrations of the unlabelled competing peptides. Each experiment was performed in triplicate and repeated twice.

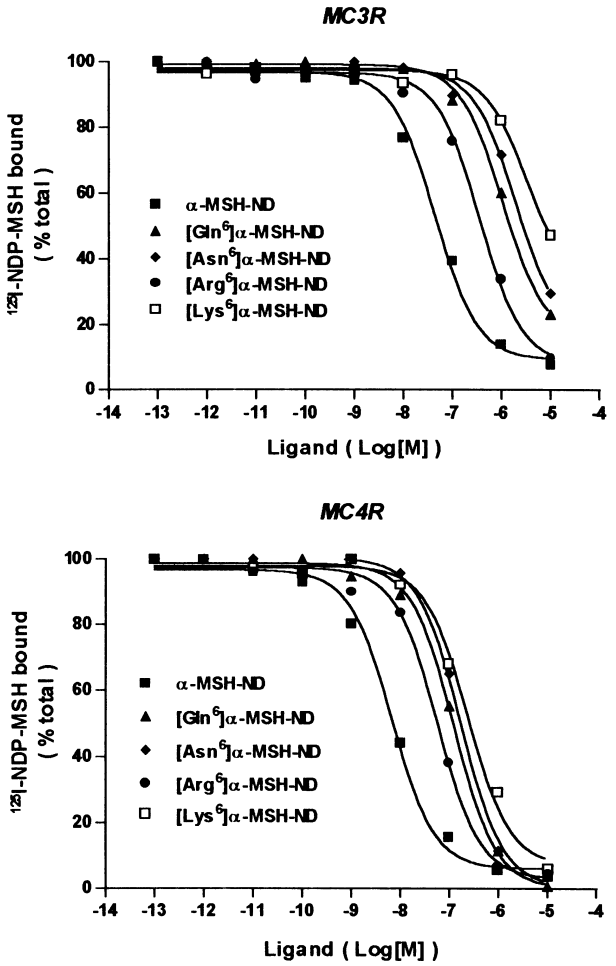

Fig. 2. Competition curves of α-MSH analogues obtained in CHO cell lines stably transfected with MC3R and MC4R using a fixed concentration of [^{125}I]NDP-MSH and varying concentrations of the unlabelled competing peptides. Each experiment was performed in triplicate and repeated twice.

Comparative study on receptor-binding activity of the synthesized peptides

To investigate if the linear form of peptide could also show certain biological activity as the cyclic form described before, we first synthesized one peptide whose sequence was the same as MTII, but being of linear form, designated α-MSH-ND. We compared its binding affinity for the MC3R and MC4R with two of the well-known MSH analogues, [Ahx4]α-MSH and

Table 2. IC_{50} values (mean ± SEM) of MSH analogues obtained from computer analysis of competition curves on MC3R and MC4R transfected CHO cells, together with the relative affinity ratios of the melanocortin receptor subtypes.

Ligand	IC_{50} (nM)		Ratio of MC3R/MC4R
	MC3R	MC4R	
NDP-MSH	0.3671 ± 0.074	0.5659 ± 0.194	0.65
[Ahx4]α-MSH	106.7 ± 32.25	238.3 ± 30.47	0.45
α-MSH-ND	47.2 ± 9.08	6.7 ± 1.07	7.04
[Gln6]α-MSH-ND	1074.0 ± 120.01	112.0 ± 25.94	9.59
[Asn6]α-MSH-ND	1998.0 ± 363.34	171.2 ± 14.81	11.67
[Arg6]α-MSH-ND	361.5 ± 57.73	57.4 ± 8.37	6.29
[Lys6]α-MSH-ND	3340.0 ± 877.05	238.1 ± 40.63	14.03
α-MSH-ND(6–10)	4730.0 ± 1180.93	827.0 ± 208.73	5.72
[Gln6]α-MSH-ND(6–10)	7156.0 ± 5063.46	1297.0 ± 392.28	5.52
[Asn6]α-MSH-ND(6–10)	6712.0 ± 4169.22	1304.0 ± 378.47	5.15

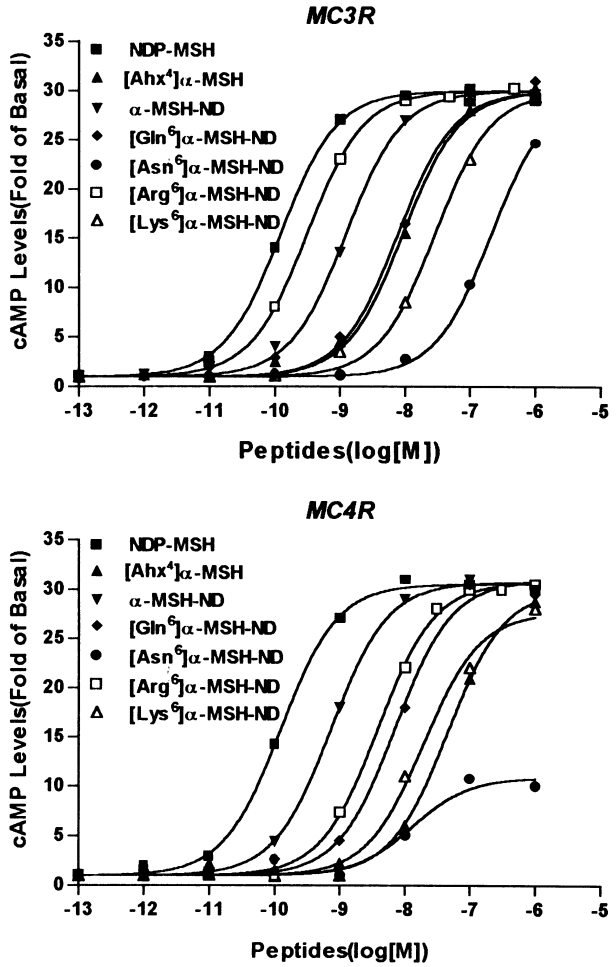

Fig. 3. Measurement of intracellular cAMP in response to increasing concentration of α-MSH analogues in CHO cell lines stably transfected with MC3R and MC4R. Each experiment was performed in triplicate and repeated twice.

NDP-MSH. As shown in Fig. 1, for MC3R, the preferential order, NDP-MSH > α-MSH-ND > [Ahx4]α-MSH, is shown with the IC_{50} values (nM) being 0.367 ± 0.074, 47.20 ± 9.08 and 106.70 ± 32.25, respectively. For MC4R, the same preferential order, NDP-MSH (0.566 ± 0.194) > α-MSH-ND (6.70 ± 1.07) > [Ahx4]α-MSH (238.30 ± 30.47), was obtained. Although without the N-terminal three amino acid residues as maintained in [Ahx4]α-MSH, α-MSH-ND still revealed a higher binding affinity for both receptors than [Ahx4]α-MSH.

Based on the data obtained for α-MSH-ND, we truncated the N-terminal Ahx4 and Asp5 residues of α-MSH-ND and substituted its His6 residue by Gln or Asn. Then we tested the binding affinity of these short peptides of truncated forms. As a result, the truncated peptides revealed lower affinities for the receptors than those untruncated substitutes (as seen in Table 2). Regarding [Gln6]α-MSH-ND(6–10) and [Asn6]α-MSH-ND(6–10), even though at the highest concentration (10^{-5} M), the displaced [^{125}I]NDP-MSH were only 33.91% and 21.37%, respectively. The IC_{50} values (nM) for the MC3R were shown as: α-MSH-ND(6–10), 4730.00 ± 1180.93, [Gln6]α-MSH-ND(6–10), 7156.00 ± 5063.46, and [Asn6]α-MSH-ND(6–10), 6712.00 ± 4169.22, and for the MC4R, 827.00 ± 208.73, 1297.00 ± 392.28 and 1304.00 ± 378.47, respectively. To define further the role of the amino acid in position 6 of α-MSH-ND in receptor-binding activity, we also substituted His6 with Gln, Asn, Arg, and Lys, respectively, and tested the binding affinities for the melanocortin receptors. As shown in Fig. 2 (IC_{50} values shown in Table 2), all of the substitutions at position 6 resulted in decreased binding affinities for both receptors. In addition, the MC3R-binding activity exhibited a different preference in the order α-MSH-ND > [Arg6]α-MSH-ND > [Gln6]α-MSH-ND > [Asn6]α-MSH-ND > [Lys6]α-MSH-ND with their IC_{50} values (nM) being 47.20 ± 9.08, 361.50 ± 57.73, 1074.00 ± 120.01, 1998.00 ± 363.34 and 3340.00 ± 877.05, respectively. In addition, for MC4R, the preferential order was the same as for MC3R: IC_{50} values (nM) were 6.70 ± 1.07, 57.40 ± 8.37, 112.00 ± 25.94, 171.20 ± 14.81 and 214.50 ± 40.63, respectively.

After calculating the ratio of IC_{50}MC3R/IC_{50}MC4R, it was found that [Lys6] α-MSH-ND exhibited the most selective activity for MC4R. The ratio order of these peptides was [Lys6]α-MSH-ND > [Asn6]α-MSH-ND > [Gln6]α-MSH-ND > α-MSH-ND > [Arg6]α-MSH-ND > α-MSH-ND(6–10), [Gln6] α-MSH-ND(6–10), [Asn6]α-MSH-ND(6–10) > NDP-MSH and [Ahx4]α-MSH, and the corresponding ratio values were 14.03, 11.67, 9.59, 7.04, 6.29, 5.72, 5.52, 5.15, 0.65 and 0.45, respectively.

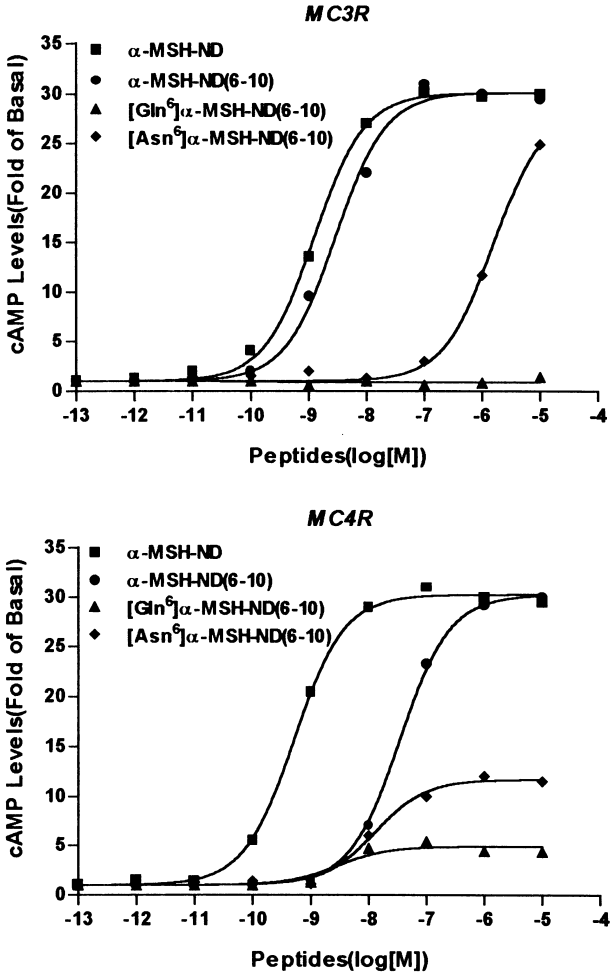

Fig. 4. Measurement of intracellular cAMP in response to increasing concentration of the α-MSH analogues in CHO cell lines stably transfected with MC3R and MC4R. Each experiment was performed in triplicate and repeated twice.

Effects of the synthesized peptides on cyclic AMP accumulation in CHO cells stably expressing MC3R or MC4R

Fig. 3 shows the receptor-mediated cAMP response of the peptides at the MC3R and MC4R, except those in truncated form: NDP-MSH also showed the highest potency of cAMP generation for both the MC3R- and MC4R-expressing CHO cells. [Arg6]α-MSH-ND exhibited higher potency than α-MSH-ND at the MC3R, which was different from the binding assay data shown above, but still lower than α-MSH-ND at the MC4R, which was identical to the receptor-binding results. In this study, [Asn6]α-MSH-ND displayed the weakest potency of cAMP generation at the MC3R of all these peptides, while being incapable of generating the maximum cAMP response at the MC4R, like the other peptides. The potency order of all the peptides tested was, at the MC3R, NDP-MSH > [Arg6] α-MSH-ND > α-MSH-ND > [Ahx4]α-MSH, [Gln6]α-MSH-ND > [Lys6]α-MSH-ND > [Asn6]α-MSH-ND; and at the MC4R, NDP-MSH > α-MSH-ND > [Arg6]α-MSH-ND > [Gln6]α-MSH-ND > [Lys6]α-MSH-ND > [Ahx4]α-MSH, > [Asn6]α-MSH-ND. The saturable stimulation of cAMP generation of [Asn6]α-MSH-ND in the MC4R, however, only showed about one-third of the stimulation of the other ligands.

With regard to the truncated forms of peptides, as shown in Fig. 4, they also displayed interesting results. Among them, α-MSH-ND(6–10) gave a comparatively good cAMP response, especially at the MC3R, exhibiting a high cAMP-generating activity almost the same as that of α-MSH-ND when concentratrion was high enough (10^{-5} M). However, substitutions of His6 with Gln or Asn resulted in a highly significant decrease in their ability to stimulate cAMP formation, and could not give rise to good activity even at a high concentration (10^{-5} M). In particular, the His6/Asn6 exchange led to a loss of all biological activity at the MC3R, and caused an almost complete loss of activity at the MC4R. As seen in Fig. 4, [Gln6]α-MSH-ND(6–10) and [Asn6]α-MSH-ND(6–10) only showed about on-sixth and one-third of maximum stimulation

Table 3. EC_{50} values (mean ± SEM) of MSH analogues obtained from computer analysis of dose–response curves on MC3R and MC4R transfected CHO cells, together with the relative bioactivity ratios of the melanocortin receptor subtypes. –, The mature cAMP generation failed to reach the maximum stimulation as shown by other ligands.

Ligand	EC_{50} (nM)		Ratio of MC3R/MC4R
	MC3R	MC4R	
NDP-MSH	0.174 ± 0.052	0.126 ± 0.020	1.381
[Ahx4]α-MSH	9.362 ± 1.932	46.040 ± 4.799	0.203
α-MSH-ND	1.523 ± 0.707	0.780 ± 0.405	1.953
[Gln6]α-MSH-ND	9.383 ± 4.620	7.880 ± 1.818	1.191
[Asn6]α-MSH-ND	271.800 ± 21.948	–	–
[Arg6]α-MSH-ND	0.381 ± 0.157	4.858 ± 0.949	0.078
[Lys6]α-MSH-ND	29.560 ± 11.525	19.890 ± 4.024	1.486
α-MSH-ND(6–10)	5.935 ± 5.260	40.050 ± 15.272	0.148

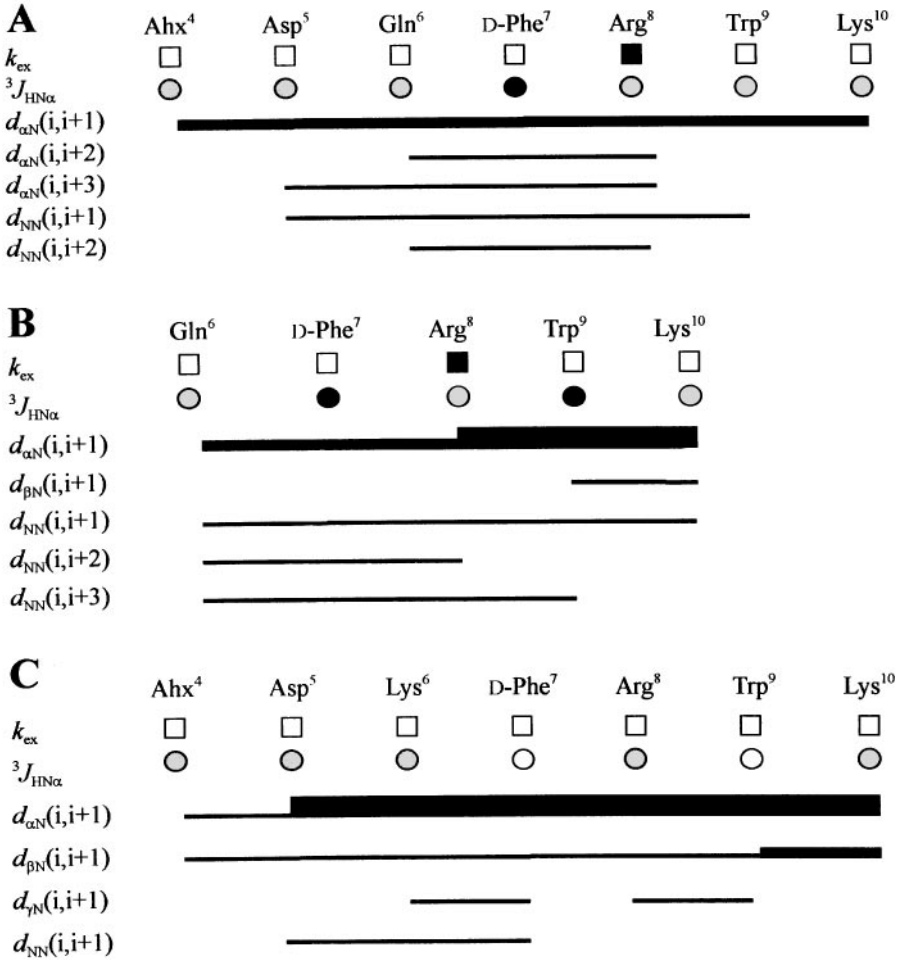

Fig. 5. Summary of NMR data for [Gln6]α-MSH-ND (A), [Gln6]α-MSH-ND (6–10) (B) and [Lys6]α-MSH-ND (C) showing the sequential and short-range NOE connectivity. Amide proton exchange rate (■, amide protons that survived for ≈ 20 h; □, amide protons that were not detected after 10 min) and backbone NH-CαH vicinal coupling constants (●, $^3J_{HN\alpha} < 6$Hz; shaded circle, 6.5Hz < $^3J_{HN\alpha} \leq 8$Hz; ○, $^3J_{HN\alpha} > 8$Hz).

Table 4. Proton NMR chemical shift assignments and temperature coefficients for [Gln6]α-MSH-ND, [Gln6]α-MSH-ND(6–10) and [Lys6]α-MSH-ND in 90% H_2O/10% D_2O. Chemical shifts are expressed relative to internal sodium 4,4-dimethyl-4-silapentane 1-sulfonate. The samples were maintained at 10 °C, pH 7.0. The temperature coefficient values were calculated using the equation $\Delta(\delta NH)/\Delta T \times 10^{-3}$.

Peptides	Residues	NH	CαH	CβH	Others	p.p.b./K
[Gln6]α-MSH-ND	Ahx4	8.44	4.13	1.58	CγH_2(1.58) CδH_3(1.13)	−5.9
	Asp5	8.58	4.53	2.71		+0.8
	Gln6	8.22	4.27	2.09, 2.18	CγH_2(1.89) NεH_2(6.96, 7.58)	−7.3
	D-Phe7	8.61	4.54	3.07, 3.16	2,6H(7.32) 4H(7.36) 3,5H (7.43)	−6.4
	Arg8	8.37	4.12	1.41	CγH_2(0.98) CδH_2(2.99) NεH(7.20)	−1.4
	Trp9	8.27	4.66	3.40, 3.37	2H(7.35) 4H(7.72) 5H(7.22) 6H(7.29) 7H(7.54) NH(10.28)	−6.8
	Lys10	8.07	4.15	1.56	CγH_2(1.34) CδH_2(1.62) CεH_2(2.879) NH_3^+(7.64)	−6.8
[Gln6]α-MSH-ND(6–10)	Gln6	8.36	4.38	1.86, 1.94	CγH_2(2.14) NεH_2(7.55, 6.96)	+0.2
	D-Phe7	8.73	4.63	3.10, 3.04	2,6H(6.93) 3,5H(7.34) 4H(7.01)	−6.0
	Arg8	8.40	4.14	1.57, 1.40	CγH_2(1.12, 1.00) CδH_2(3.00) NεH(7.11)	+0.6
	Trp9	8.23	4.71	3.37	2H(7.32) 4H(7.69) 5H(7.18) 6H(7.26) 7H(7.51) NH(10.22)	−6.2
	Lys10	8.00	4.14	1.75, 1.62	CγH_2(1.28) CεH_2(2.98) NH_3^+(7.58)	−7.2
[Lys6]α-MSH-ND	Ahx4	8.31	3.88	1.43	CγH_2(1.43) CδH_3(0.98, 1.09)	−6.1
	Asp5	8.50	4.38	2.83, 2.77		−7.4
	Lys6	8.14	4.11	1.72, 1.65	CγH_2(1.26, 1.18) CδH_2(1.57, 1.65) CεH_2(2.88) NH_3^+(7.56)	−5.9
	D-Phe7	8.52	4.40	3.05, 3.08	2,6H(7.25) 3,5H(7.36) 4H(7.30)	−6.2
	Arg8	8.40	3.94	1.19	CγH_2(0.77) CδH_2(2.97) NεH(7.10)	−5.0
	Trp9	8.18	4.44	3.31	2H(7.08) 4H(7.51) 5H(7.13) 6H(7.21) 7H(7.31) NH(10.09)	−7.7
	Lys10	8.06	3.94	1.48	CγH_2(1.00) CδH_2(1.35) C$^{\varepsilon}$$H_2$(2.92) NH_3^+(7.56)	−7.1

of α-MSH-ND and α-MSH-ND(6–10). The corresponding EC_{50} values of these α-MSH analogues are given in Table 3.

NMR resonance assignments and secondary structures of α-MSH analogues

Complete proton resonance assignment followed standard sequential analysis [29] based on two-dimensional TOCSY and NOESY spectra collected in H_2O solution. Chemical shifts and temperature coefficients of [Gln6]α-MSH-ND, [Gln6]α-MSH-ND(6–10) and [Lys6]α-MSH-ND peptides are summarized in Table 4. The data of hydrogen exchange of three α-MSH analogues are displayed in Fig. 5. The NH protons Arg8 in both [Gln6]α-MSH-ND and [Gln6]α-MSH-ND(6–10) exhibited slower hydrogen exchange rates, suggesting a manifestation of a better-protected amide proton, in other words, a folded structure for this region. However, all backbone amide protons of [Lys6]α-MSH-ND were exchanged quickly.

The sequential and short-range NOE connectivities for three α-MSH analogues are summarized in Fig. 5. In [Gln6] α-MSH-ND, a $d_{\alpha N}(i,i+3)$ NOE indicative of β-turn conformation was observed between Asp5 and Arg8. This finding was also supported by $d_{\alpha N}(i,i+2)$ and $d_{NN}(i,i+2)$ NOEs together with a small vicinal $^3J_{HN\alpha}$ coupling constant of D-Phe7 (< 6Hz). The chemical shift differences [30] of Cα protons of [Gln6]α-MSH-ND were computed using the random coil values and showed significant deviations for residues of Asp5 [0.51 p.p.m. (± 0.10)] and Arg8 [0.54 p.p.m. (± 0.10)], respectively. This data supported the notion that [Gln6] α-MSH-ND has a propensity to form a type I′ β-turn, which is a mirror image corresponding to a type I β-turn, around Asp5–Gln6–DPhe7–Arg8.

Figure 5B shows the sequential and short-range NOE connectivity of [Gln6]α-MSH-ND(6–10). A number of short-range NOEs were detected around the message sequence of the peptide. The stretch of medium $d_{\alpha N}(i,i+1)$ NOEs for Gln6–Arg8 were observed; however, neither the $d_{\alpha N}(i,i+2)$ nor $d_{\alpha N}(i,i+3)$, NOEs indicative of stable tight β-turns, were detected. On the basis of a $d_{NN}(i,i+2)$ between Gln5 and Arg8 together with a small $^3J_{HN\alpha}$ coupling constant of D-Phe7 residue, [Gln6]α-MSH-ND(6–10) adopted a γ-turn conformation composed of three residues Gln6-D-Phe7-Arg8. This data is also supported by the temperature coefficients and hydrogen exchange data of [Gln6]α-MSH-ND(6–10) (Table 4 and Fig. 5B). In addition,

Table 5. Torsion angles ϕ and ψ (degress) for central residues in turn conformations of three α-MSH analogues. Torsion angles of α-MSH analogues were measured from the average REM structure. The central residue involved in γ-turn is i + 1; the two residues for β-turn are i + 1 and i + 2, respectively.

		Torsion angles			
Peptides	Central residues	ϕ_{i+1}	ψ_{i+1}	ϕ_{i+2}	ψ_{i+2}
[Gln6]α-MSH-ND	Gln6/D-Phe7	64	33	86	−10
[Gln6]α-MSH-ND(6–10)	D-Phe7	−75	58		
[Lys6]α-MSH-ND	Lys6/D-Phe7	−106	−170	−36	−91

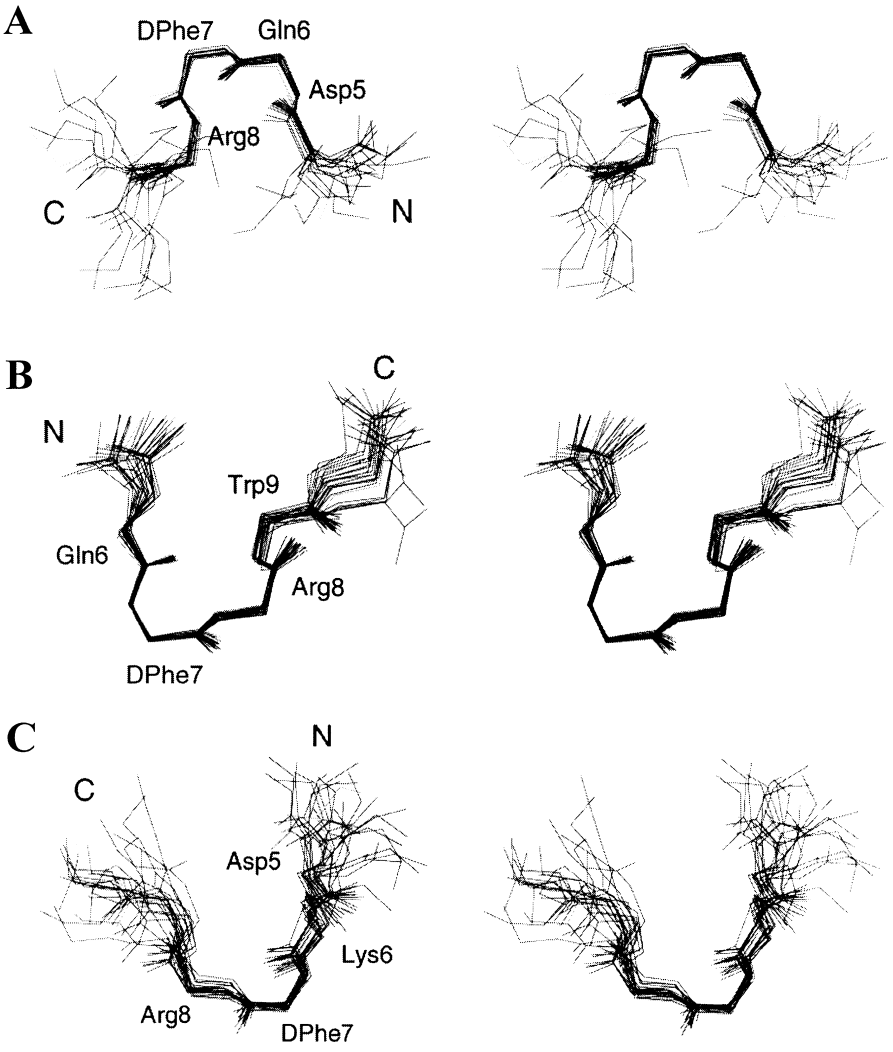

Fig. 6. Final simulated-annealing structures of [Gln6]α-MSH-ND (A), [Gln6]α-MSH-ND (6–10) (B) and [Lys6]α-MSH-ND (C). Superposition of the final $<SA>_k$ structures (thin line) (16, 27 and 21 structures for [Gln6]α-MSH-ND, [Gln6]α-MSH-ND(6–10) and [Lys6]α-MSH-ND, respectively) over the average REM structure (thick line) displayed in stereoview. All backbone atoms of three α-MSH analogues are superimposed from Asp4 to Arg8 except for [Gln6]α-MSH-ND(6–10) (from Gln6 to Arg8).

the deviations from random coil chemical shifts for the CαH resonances suggested the existence of a secondary structural element for [Gln6]α-MSH-ND(6–10).

For [Lys6]α-MSH-ND, short-range NOEs for turn conformation around the message sequence were not observed (Fig. 5C). Most residues in this peptide showed the large $^3J_{HN\alpha}$ as well as a rapid exchange of NH protons.

Solution structures of [Gln6]α-MSH-ND, [Gln6]α-MSH-ND(6–10) and [Lys6]α-MSH-ND

Using the experimental constraints from NMR data, 30 structures of all α-MSH analogues were calculated by distance geometry followed by a simulated-annealing method. The quality of the final structures was estimated on the grounds of the number of constraint violations, minimal energy and error factors based on geometry and constraints. Among the simulated annealing structures ($<SA>_k$), 16 of [Gln6]α-MSH-ND, 27 of [Gln6]α-MSH-ND(6–10) and 21 of [Lys6] α-MSH-ND demonstrated no constraint violations greater than 0.03 nm for distances and 3 ° for torsion angles. Each average structure was calculated from the geometrical average of final structures and followed the restraints energy minimization (REM) procedure. The backbone conformations are superimposed from Asp5 to Arg8 (Fig. 6A) and the average REM structure ($<\overline{SA}>_{kr}$) of [Gln6] α-MSH-ND showed a 0.042 nm rmsd value for backbone heavy atoms with respect to 16 $<SA>_k$ structures. All of the structures displayed small deviations from idealized covalent geometry. An inspection of the $<\overline{SA}>_{kr}$ structure clearly showed that [Gln6]α-MSH-ND preferred type I′ β-turn conformation residues of Asp5–Gln6–DPhe7–Arg8. The backbone structures of [Gln6]α-MSH-ND showed a standard hydrogen bond between carbonyl oxygen of Asp5 and amide hydrogen of Arg8. This was supported by the temperature coefficients and slowly exchanged amide hydrogen data. Table 5 shows the ϕ and ψ torsion angles of the central residues for $<\overline{SA}>_{kr}$ structure. The dihedral angles measured from the $<\overline{SA}>_{kr}$ structure also supported the tight turn, which includes the residues Asp5-Gln6-D-Phe7-Arg8.

A best-fit superposition of all 27 $<SA>_k$ and $<\overline{SA}>_{kr}$ of [Gln6]α-MSH-ND(6–10) is shown in Fig. 6B. The average REM structure of [Gln6]α-MSH-ND(6–10) was very well converged for all backbone heavy atoms with respect to 27 $<SA>_k$ structures (rmsd value of 0.036 nm). All $<SA>_k$ and $<\overline{SA}>_{kr}$ structures showed a hydrogen bond between carbonyl oxygen of Gln6 and amide hydrogen of Arg8. Table 5 lists the backbone torsion angles for central residues for α-MSH analogues. This data demonstrated that the three residues Gln6–DPhe7–Arg8 of [Gln6]α-MSH-ND(6–10) adopted a reverse γ-turn conformation.

Fig. 6C shows the superposition of the final 21 $<SA>_k$ structures of [Lys6]α-MSH-ND over $<\overline{SA}>_{kr}$. The rmsd of $<SA>_k$ structures for backbone atoms was 0.058 nm to $<\overline{SA}>_{kr}$ structures. The backbone torsion angles for all 21 $<SA>_k$ structures indicated that all ϕ and ψ values were distributed in energetically acceptable regions. For [Lys6] α-MSH-ND, a turn conformation appeared comprising the residues Asp5-Lys6-D-Phe7-Arg8. The peptide formed a right angle twist to make a bend conformation. This conformation distorted the orientation of Asp5 and resulted in the weak hydrogen bond between the carbonyl oxygen of Asp5 and amide hydrogen of Arg8. NOEs around the message sequence for the standard β-turn were not observed and all residues showed the large $^3J_{HN\alpha}$ together with a fast hydrogen exchange rate for all backbone amide protons.

DISCUSSION

During states of positive energy balance, the adipose mass expands, leptin concentrations increases, and the resulting output from the brain favours reduced food intake and a reduction in the size of the adipose mass [31]. The melanocortin neurone appears to be a target of leptin action because leptin receptors are expressed on POMC neurones in the arcuate nucleus [32]. Recent reports with knockout techniques [33,34] and intracerebroventricular injection of the cyclic MSH analogues SHU9119 and MTII [12] linked the MC4R to feeding behaviour and weight homeostasis. MC3Rs are also abundantly expressed in the brain and peripheral tissues such as placenta, gut tissues and the human heart [14]. The physiologic roles of the MC3R, however, are not yet fully understood. Until now, most of the known melanocortin analogues have shown only minimal discrimination between the MC3R and the MC4R [17]. As MC4R-selective substances have been considered as potential candidates for the treatment of eating disorders, including obesity and anorexia, any analogue which shows significant discrimination will be worthwhile for studying the physiologic roles of melanocortin receptor subtypes and for studying the structures and functions of α-MSH analogues.

All of the natural melanocortins contain the conserved core structure (i.e. His6-Phe7-Arg8-Trp9), and each of the core residues has been thought to exhibit an important effect for biological activity [35–38]. A cyclic form of MTII (Ac-Ahx-cyclic[Asp-His-(D-Phe)-Arg-Trp-Lys]-NH_2) has been designed as a lead compound for structure–function studies on human melanocortin receptors [39]. In our previous NMR study, α-MSH formed a hairpin loop conformation, whereas α-MSH-ND, a linear form of MTII, preferred a type I β-turn comprising the residues Asp-His6-(D-Phe7)-Arg8 [19]. To further investigate the role of type I β-turn and to make shorter analogues, we truncated the N-terminal Ahx4 and Asp5 residues of α-MSH-ND and substituted the His6 residue with Gln or Asn residue, and then observed the structural traits of [Gln6]α-MSH-ND(6–10) by NMR. Truncation of Ahx4 and Asp5 of α-MSH-ND decreased remarkably the receptor-binding and cAMP-generating activity. [Gln6]α-MSH-ND (6–10) was almost unable to activate both receptors, even though it could bind to both receptors. In NMR study, although [Gln6]α-MSH-ND(6–10) is composed of only five amino acid residues, it still revealed a very stable structure and a tight γ-turn composed of Gln6-D-Phe7-Arg8. Therefore, a plausible explanation for the remarkable loss of the receptor-binding and cAMP-generating activity of the truncated analogues might be that these short analogues could no longer maintain a stable classic type I β-turn conformation. On the other hand, [His6]α-MSH-ND(6–10) was able to generate the maximum stimulation of the receptors at a higher concentration (10^{-5} M), whereas [Gln6]α-MSH-ND(6–10) was almost completely incapable of stimulating both receptors. This suggested that the degree of flexibility and ability of truncated analogues for receptor activation might be partially dependent on the flexible free N-terminal end of the sixth residue itself.

α-MSH-ND prefers a type I β-turn and the position of the imidazole ring of the His6 residue was displaced by the substitution of Phe7 by D-Phe7 in our previous NMR study [19]. Therefore, we changed the His6 residue of α-MSH-ND to Gln, Asn, Arg or Lys to analyse the contribution of the His6 residue on receptor binding and activation. The replacement of His6 by Asn6 and Gln6 decreased the receptor-binding activity by 22.8- and 42.3-fold for the MC3R, and by 25.6- and 16.7-fold for the MC4R, respectively. The structure of [Gln6]α-MSH-ND exhibited a stable type I′ β-turn comprising residues Asp5, Gln6, D-Phe7 and Arg8. Compared with α-MSH-ND, the substitution of His6 by Arg6 and Lys6, two positively charged residues, decreased the receptor-binding activity by 7.7- and 70.8-fold for the MC3R, and by 8.6- and 35.5-fold for the MC4R, respectively. [Arg6]α-MSH-ND showed a significantly higher binding affinity to both receptors than [Lys6]α-MSH-ND. This suggested that, for these two analogues, the different potencies were probably the result of the distinct sizes of their sixth residues rather than the electrical charge. Of the substituted peptides, [Lys6]α-MSH-ND showed the lowest binding affinity and a greatly decreased cAMP-generating activity. Even for the MC4R, the binding affinity of [Lys6]α-MSH-ND decreased ≈ 36-fold compared with that of α-MSH-ND. In NMR, [Lys6]α-MSH-ND demonstrated a γ-turn like conformation around Lys6-DPhe7-Arg8. These dramatic changes of binding affinity shown above could be explained easily from our structural studies. Taken together, our results suggested that the type I β-turn could affect both potencies and prolonged biological activity of melanotropin peptides.

In this study, the preference order of receptor affinities of NDP-MSH, α-MSH-ND and [Ahx4]α-MSH for both the MC3R and the MC4R was NDP-MSH > MTII ≈ α-MSH-ND > [Ahx4]α-MSH, in which the MTII data was obtained from Schiöth [36]. The higher receptor-binding activity compared to the truncated analogues suggested that the N or C terminus of NDP-MSH may play a certain role in both the binding affinity and selectivity for MC4R. Recently, Schiöth *et al*. also reported that the C terminus was more important than the N terminus for binding to the MC4R after comparing NDP-MSH(1–9) and NDP-MSH(4–13) [40]. NDP-MSH, even MTII and α-MSH-ND, of which Phe7 is substituted by D-Phe7, showed a remarkably higher MC4R-selective affinity and potency in receptor activation compared with [Ahx4]α-MSH, whereas all of the His6-substituted α-MSH-ND analogues still preserved MC4R preference in receptor-binding activity. In contrast, Ahx4-and Asp5-truncated α-MSH-ND(6–10) showed the loss of MC4R preference in cAMP-generating activity. Loss of MC4R preference in cAMP-generating activity was also observed in [Arg^6]α-MSH-ND. Although the different biological activity of these analogues for the MC3R and the MC4R may arise not only due to the subtype differences, but also due to species difference, these findings, taken together, support the previous observation that the substitution of Phe7 by D-Phe7 could be decisive in maintaining high receptor activation and in obtaining MC4R selectivity by enhancing hydrophobic interaction [16,17,41,42]. It may also suggest that the sixth residue of α-MSH analogues is important for selective receptor activation.

In conclusion, we have shown that a type I β-turn backbone structure comprising the residues Asp5-His6-(D-Phe7)-Arg8 is important for receptor binding and activation, as well as the selectivity of α-MSH analogues. Therefore, a potent MC4R-selective substance could be developed by extensive modifications of core residues, while preserving the type I β-turn structure.

ACKNOWLEDGEMENTS

This work was supported by a research grant from the Korea Ministry of Health and Welfare (HMP-98-D-4-0033) (1998). We thank R. D. Cone, Vollum Institute for Advanced Biomedical Research, Portland, OR, USA for supplying the rMC3R and hMC4R cDNAs inserted in expressing vectors. We also thank R. Ross for English language revision.

REFERENCES

1. De Wied, D. & Jolles, J. (1982) Neuropeptides derived from pro-opiomelanocortin: behavioral, physiological and neurochemical effects. *Physiol. Rev.* **62**, 976–1059.
2. Campfield, L.A., Smith, F.J. & Burn, P. (1998) Strategies and potential molecular targets for obesity treatment. *Science* **280**, 1383–1387.
3. Chhajlani, V., Muceniece, R. & Wikberg, J.E.S. (1993) Molecular cloning and expression of the human melanocyte stimulating hormone receptor. *Biochem. Biophys. Res. Commun.* **195**, 866–873.
4. Chhajlani, V. & Wikberg, J.E.S. (1992) The cloning of a family of genes that encode the melanocortin receptors. *FEBS Lett.* **309**, 417–420.
5. Gantz, I., Konda, Y., Tashiro, T., Shimoto, Y., Miwa, H., Munzert, G., Watson, S.J., DelValle, J. & Yamada, T. (1993) Molecular cloning of a novel melanocortin receptor. *J. Biol. Chem.* **268**, 8246–8250.
6. Gantz, I., Miwa, H., Konda, Y., Shimoto, Y., Tashiro, T., Watson, S.J., DelValle, J. & Yamada, T. (1993) Molecular cloning, expression and gene localization of a fourth melanocortin receptor. *J. Biol. Chem.* **268**, 15174–15179.
7. Mountjoy, K.G., Robbins, L.S., Mortrud, T.T. & Cone, R.D. (1992) The cloning of a family of genes that encode the melanocortin receptors. *Science* **257**, 1248–1251.
8. Krude, H., Bieberann, H., Luck, W., Hom, R., Brabant, G. & Gruters, A. (1998) Severe early-onset obesity, adrenal insufficiency and red hair pigmentation caused by POMC mutation in humans. *Nat. Genet.* **19**, 155–157.
9. Huszar, D., Lynch, C.A., Fairchild-Huntress, V., Dunmore, J.H., Fang, Q., Berkemeier, L.R., Gu, W., Kesterson, R.A., Boston, B.A., Cone, R.D., Smith, F.J., Campfield, L.A., Burn, P. & Lee, F. (1997) Targeted disruption of the melanocortin-4 receptor results in obesity in mice. *Cell* **88**, 131–141.
10. Bultman, S.J., Michaud, E.J. & Woychik, R.P. (1992) Molecular characterization of the mouse agouti locus. *Cell* **71**, 1195–1204.
11. Graham, M., Shutter, J.R., Sarmiento, U., Sarosi, I. & Stark, K.L. (1997) Overexpression of agrt lead to obesity in transgenic mice. *Nat. Genet.* **17**, 273–274.
12. Fan, W., Boston, B.A., Kesterson, R.A., Hruby, V.J. & Cone, R.D. (1997) Role of melanocortinergic neurons in feeding and the *agouti* obesity syndrome. *Nature* **385**, 165–168.
13. Cone, R.D., Lu, D., Koppula, S., Vage, D.I., Klungland, H., Boston, B., Chen, W., Orth, D.N., Pouton, C. & Kesterson, R.A. (1996) The melanocortin receptors: agonists, antagonists, and the hormonal control of pigmentation. *Recent Prog. Horm. Res.* **51**, 287–317.
14. Mountjoy, K.G. & Wong, J. (1997) Obesity, diabetes and functions for pro-opiomelanocortin-derived peptides. *Mol. Cell. Endocrinol.* **128**, 171–177.
15. Sawyer, T.K., Sanfilippo, P.J., Hruby, V.J., Engel, M.H., Heward, C.B., Burnett, J.B. & Hadley, M.E. (1980) 4-Norleucine, 7-D-pheylalanine-alpha-melanocyte-stimulating hormone: a highly potent alpha-melanotrophin with ultralong biological activity. *Proc. Natl Acad. Sci. USA* **77**, 5754–5758.
16. Chaturvedi, D.N., Knittel, J.J., Hruby, V.J., Castrucci, A.M. & Hadley, M.E. (1984) Synthesis and biological actions of highly potent and prolonged acting biotin-labeled melanotropins. *J. Med. Chem.* **27**, 1406–1410.
17. Schiöth, H.B., Muceniece, R., Mutulis, F., Prusis, P., Lindeberg, G., Sharma, S.D., Hruby, V.J. & Wikberg, J.E. (1997) Selectivity of cyclic [D-Nal^7] and [D-Phe^7] substituted MSH analogues for the melanocortin receptor subtypes. *Peptides* **18**, 1009–1013.
18. Schiöth, H.B., Muceniece, R. & Wikberg, J.E. (1997) Selectivity of [Phe-1^7], [Ala^6] and [D-Ala^4, Gln^5, Tyr^6]substituted ACTH (4-10) analogues for the melanocortin receptors. *Peptides* **18**, 761–763.
19. Lee, J.H., Lim, S.K., Huh, S.H., Lee, D. & Lee, W. (1998) Solution structures of the melanocyte-stimulating hormones by two-dimensional NMR spectroscopy and dynamical simulated-annealing calculation. *Eur. J. Biochem.* **257**, 31–40.
20. Davis, D.G. & Bax, A. (1985) Assignment of complex ^{1}H NMR spectra via two-dimensional homonuclear Hartmann-Hahn spectroscopy. *J. Am. Chem. Soc.* **107**, 2820–2821.
21. Jeener, J., Meier, B.H., Bachman, P. & Ernst, R.R. (1979) Investigation of exchange processes by two-dimensional NMR spectroscoopy. *J. Chem. Phys.* **71**, 4546–4553.
22. Rance, M., Sorensen, O.W., Bodenhausen, G., Wagner, G., Ernst, R.R. & Wuthrich, K. (1983) Improved spectral resolution in COSY ^{1}H-NMR spectra of proteins via double quantum filtering. *Biochem. Biophs. Res. Commun.* **117**, 479–485.
23. Marion, D. & Wuthrich, K. (1983) Application of phase sensitive two-dimensional correlated spectroscopy (COSY) for measurements of ^{1}H-^{1}H spin-spin coupling constants in proteins. *Biochem. Biophs. Res. Commun.* **113**, 967–974.
24. Otting, G., Widmer, H., Wagner, G. & Wuthrich, K. (1986) Origin of t_1 and t_2 ridges in 2D NMR spectra and procedures for suppression. *J. Magn. Reson.* **66**, 187–193.
25. Nilges, M., Clore, G.M. & Gronenborn, A.M. (1988) Determination of three-dimensional structures of proteins from interproton distance data by hybrid distance geometry-dynamical simulated annealing calculations. *FEBS Lett.* **229**, 317–324.
26. Nilges, M., Gronenborn, A.M., Brunger, A.T. & Clore, G.M. (1988) Determination of three-dimensional structures of proteins by simulated annealing with interproton distance restraints. Application to crambin, potato carboxypeptidase inhibitor and barley serine proteinase inhibitor 2. *Protein Eng.* **2**, 27–38.
27. Lee, W., Moore, C.H., Watt, D.D. & Krishna, N.R. (1994) Solution structure of the variant-3 neurotoxin from *Centruroides sculpturatus* Ewing. *Eur. J. Biochem.* **218**, 89–95.
28. Wuthrich, K., Billeter, M. & Braun, W. (1983) Pseudo-structures for the 20 common amino acids for use in studies of protein conformations by measurements of intramolecular proton-proton distance constraints with nuclear magnetic resonance. *J. Mol. Biol.* **169**, 949–961.
29. Wuthrich, K. (1986) *NMR of Proteins and Nucleic Acids*. Wiley, New York, USA.
30. Wishart, D.S., Sykes, B.D. & Richards, F.M. (1992) The chemical shift index: a fast and simple method for the assignment of protein secondary structure though NMR spectroscopy. *Biochemistry.* **31**, 1647–1651.
31. Friedan, J.M. (1997) The alphabet of weight control. *Nature* **385**, 119–121.
32. Woods, S.C., Seeley, R.J., Porte,D. Jr & Schwartz, M.W. (1998) Signals that regulated food intake and energy homeostasis. *Science* **280**, 1378–1383.
33. Kask, A., Rago, L., Korrovits, P., Wikberg, J.E. & Schiöth, H.B. (1998) Evidence that orexigenic effects of melanocortin 4 receptor antagonist HS014 are mediated by neuropeptide Y. *Biochem. Biophys. Res. Commun.* **248**, 245–249.
34. Kesterson, R.A., Huszar, D., Lynch, C.A., Simerly, R.B. & Cone, R.D. (1997) Induction of neuropeptide Y gene expression in the dorsal medial hypothalamic nucleus in two models of the agouti obesity syndrome. *Mol. Endocrinol.* **11**, 630–637.
35. Eberle, A.N. (1988) *The Melanotropin: Chemistry, Physiology and Mechanisms of Action*. Karger, Basle.

36. Schiöth, H.B., Muceniece, R., Wikberg, J.E. & Chhajlani, V. (1995) Characterization of melanocortin receptor subtypes by radioligand binding analysis. *Eur. J. Pharmcol.* **288**, 311–317.
37. Schiöth, H.B., Muceniece, R. & Wikberg, J.E. (1996) Characterization of the melanocortin 4 receptor by radioligand binding. *Pharmacol. Toxicol.* **79**, 161–165.
38. Schiöth, H.B., Muceniece, R., Larsson, M., Mutulis, F., Szardenings, M., Prusis, P., Lindeberg, G. & Wikberg, J.E. (1997) Binding of cyclic and linear MSH core peptides to the melanocortin receptor subtypes. *Eur. J. Pharmcol.* **319**, 369–373.
39. Al-Obeidi, F., Castrucci, A.L., Hadley, M.E. & Hruby, V.J. (1989) Potent and prolonged acting cyclic lactam analogues of α-melanotropin: Design based on molecular dynamics. *J. Med. Chem.* **32**, 2555–2561.
40. Schiöth, H.B., Mutulis, F., Muceniece, R., Prusis, P. & Wikberg, J.E. (1998) Selective properties of C- and N-terminals and core residues of the melanocyte-stimulating hormone on binding to the human melanocortin receptor subtypes. *Eur. J. Pharmol.* **349**, 359–366.
41. Nikiforovich, G.V., Sharma, S.D., Hadley, M.E. & Hruby, V.J. (1997) Studies of conformational isomerism in alpha-melanocyte stimulating hormone by design of cyclic analogues. *Biopolymers* **46**, 155–167.
42. Haskell-Luevano, C., Nikiforovich, G.V., Sharma, S.D., Yang, Y.K., Dickinson, C., Hruby, V.J. & Gantz, I. (1997) Biological and conformational examination of stereochemical modifications using the template melanotropin peptide, Ac-Nle-c[Asp-His-Phe-Arg-Trp-Ala-Lys]-NH_2, on human melanocortin receptor. *J. Med. Chem.* **40**, 1738–1748.